THE HIGH CURRENT EXPERIMENT: FIRST RESULTS*

Seidl, P. A. (LBNL) Baca, D. (LBNL), Bieniosek, F. M. (LBNL), Faltens, A. (LBNL), Lund, S.M. (LLNL), Molvik, A.W. (LLNL), Prost, L. R. (LBNL), Waldron, W. L. (LBNL)

LBNL: Lawrence Berkeley National Laboratory, Berkeley, CA 94720 USA

LLNL: Lawrence Livermore National Laboratory, Livermore, CA 94550 USA

Corresponding author:

Peter Seidl

Lawrence Berkeley National Laboratory, MS 47-112

One Cyclotron Road

Berkeley, CA 94720 USA

Tel: 510-486-7653

Fax: 510-486-5392

E-mail: paseidl@lbl.gov

Short title: THE HIGH CURRENT EXPERIMENT: FIRST RESULTS

22 manuscript pages 1 table 7 figures

---

* Supported by the Office of Energy Research, US DOE, at LBNL and LLNL under contract numbers DE-AC03-76SF00098 and W-7405-Eng-48.

Abstract

The High Current Experiment (HCX) is being assembled at Lawrence Berkeley National Laboratory as part of the US program to explore heavy-ion beam transport at a scale representative of the low-energy end of an induction linac driver for fusion energy production. The primary mission of this experiment is to investigate aperture fill factors acceptable for the transport of space-charge dominated heavy-ion beams at high space-charge intensity (line-charge density ~ 0.2 μC/m) over long pulse durations (>4 μs). This machine will test transport issues at a driver-relevant scale resulting from nonlinear space-charge effects and collective modes, beam centroid alignment and beam steering, matching, image charges, halo, lost-particle induced electron effects, and longitudinal bunch control. We present the first experimental results carried out with the coasting K^+ ion beam transported through the first 10 electrostatic transport quadrupoles and associated diagnostics. Later phases of the experiment will include more electrostatic lattice periods to allow more sensitive tests of emittance growth, and also magnetic quadrupoles to explore similar issues in magnetic channels with a full driver scale beam.

Keywords: inertial fusion energy, heavy-ion fusion, linear accelerators, space-charge, phase space

1 INTRODUCTION

The Heavy-Ion-Fusion (HIF) Program's objective is to provide a comprehensive scientific knowledge base for inertial fusion energy (IFE) driven by high-brightness heavy-ion beams. Filling the apertures as much as possible is very important in multi-beam induction linacs in order to minimize the transverse cross-sectional area of multi-beam focusing arrays. Thus, it is important to maximize the beam current density over the cross-section of the array. The optimum number of channels and the size of each channel be linked to the choice of beam parameters and focusing technology. The HCX will explore intense-beam transport limits at a scale characteristic of the low-energy end of a multi-beam induction linac driver, using a single beam to save on cost. Advances in the understanding of the physics of intense ion beam transport and acceleration of a single beam will enable better determination of the optimal beam aperture filling factor and pulse duration. Small beam-edge to aperture clearances at high intensities makes it crucial to understand how various processes influence practical transport limits. These limits may be different in magnetic and electric focusing sections, and most cost-optimal driver concepts employ both electrostatic (low energy) and magnetic (higher energy) focusing sections.

The single-beam HCX is the first heavy-ion electrostatic and magnetic quadrupole transport experiment with simultaneously: high line charge density ($\lambda \approx 0.1\text{-}0.2$ μC/m), long pulse duration ($\tau > 4$ μs), and high injection energy ($1.0 < E < 1.6$ MeV, K^+, coasting beam). These parameters, for a driver, are believed to lie in the rather broad ranges: $0.1 < \lambda < 1.0$ μC/m, $5 < \tau < 50$ μs, and $1 < E < 4$ MeV at injection. Previous scaled heavy-ion transport experiments (For example: *Tiefenback*, 1987 and *Fawley et al.* 1997*)* had much

less space-charge intensity ($\lambda < 0.04$ μC/m) and were not capable of resolving scale-dependent issues in transport. A goal of the HCX is to identify and understand processes that constrain choices of machine aperture needed for high confidence, but attractive, driver designs.

We are at the early stages of this experiment, beginning with the critical matching of the injected beam to the transport lattice, preliminary transport measurements and diagnostics development.

2 PROCESSES THAT WILL LIMIT TRANSPORTABLE BEAM CURRENT

The following processes (*Seidl et al*., 2001) can limit the transportable beam current. Moreover, the deleterious effects can be enhanced at the high fill factors desirable for HIF. The objective of the HCX is to obtain data on how these processes limit transportable beam current.

(1) *Nonlinear fields*: The transverse phase space of the beam can be diluted (emittance growth) due to nonlinear fields. If the effects are significant, they will be evident in the transverse phase space measurements of the beam.

(2) *Alignment errors*: After an initial set of measurements with a well-aligned beam, we will parametrically vary the initial centroid offset of the beam in the transport lattice. The oscillations bring the beam-edge closer to the physical aperture, resulting in larger nonlinear forces due to applied-field multipoles and image charges.

(3) *Lost particles*: Beam interactions with background gas, charge exchange, and large amplitude beam halo can result in particles lost to the machine aperture. Over a long pulse, this can result in cascades of desorbed gas being released from surfaces and

production of secondary electrons that will interact with the beam pulse. The yield of desorbed atoms is expected to be large and has considerable impact on the needed aperture, but little relevant data exists to help fix needed beam edge to aperture clearances for characteristic HIF pulse durations and vacuum systems. Secondary electrons are also an issue of strong concern in magnetic quadrupole transport with the expectation that they will be trapped in the multi-kV potential well of the ion-beam leading to partial neutralization, and loss in beam quality. A diagnostic has been built that will be used to measure the secondary electron, ion, and atom yields from glancing collisions of K+ ions with beam tube walls. In the magnet bores, diagnostics are being designed to measure the density of trapped electrons (*Molvik et al.,* 2002).

(5) *Longitudinal physics*: Matching of the beam head and maintaining beam control over the pulse in the presence of acceleration and velocity tilt for compression introduces various constraints. An induction bunch control module is being built that will allow experiments in waveform correction and compensation for the longitudinal space charge at the head and tail of the beam.

In order to investigate these processes and their influence on the maximum transportable current we will increase the aperture-filling factor by decreasing the quadrupole-focusing gradient. In addition we will also be able to vary the injector beam current by ≈–15% / +40% with variations in the extraction voltage of the three-electrode gun. The resulting beam measurements will enable the design of more optimal and reliable next-generation accelerators for HIF research. These approaches to determining the aperture-filling factor will be discussed below.

3 INITIAL EXPERIMENTAL CONFIGURATION AND DIAGNOSTICS

The present configuration begins with the ion source and injector, an electrostatic quadrupole matching section, and the first 10 electrostatic transport quadrupoles. (30-40 electrostatic quadrupoles are planned for the experiment). At the end of the beam line is a multi-purpose diagnostic station (D-end). Beam diagnostics are also located at the interface of the matching section and the transport quadrupoles. The present layout of the apparatus is shown in Fig. 1. The diagnostics at QD1 are transverse slit scanners and a whole beam Faraday cup. Because the longitudinal space required by these diagnostics is considerably greater than the available drift space between the focusing elements (20 mm in the transport section), the quadrupole at QD1 slides out of the beam path to allow the intercepting beam diagnostics measurements.

The typical vacuum pressure in the matching and transport beam line is 1-2 x 10^{-7} Torr during beam measurements. The base pressure when the ion source is cold is ≈8 x 10^{-8} Torr.

Planned additions to the experiment are four pulsed magnetic quadrupoles and associated diagnostics (summer 2002), 20-30 more electrostatic transport quadrupoles (2003), and a bunch control induction module. If funding allows, we plan to do beam tests with the recently designed prototype superconducting quadrupole doublet that will be built this year (*Faltens et al.,* 2002).

3.1 Injector and matching section

The front end of the apparatus consists of the ion injector (*Kwan et al*. 2002) that delivers 1-1.8 MeV K^+ ions. The corresponding ion beam current ranges from 0.2 A to

0.6 A, and the normalized emittance of the beam at the exit of the injector is $\varepsilon_n \approx 1$ π mm-mrad. The phase space was characterized with double slit emittance scanners before adding the matching section.

All commissioning and preliminary measurements have been made at 1.0 MeV, to avoid any high voltage insulation issues in the injector. The beam energy at present is limited to 1.5 MeV until we modify the water resistor that distributes the voltage along the ESQ injector column to ensure a positive pressure in the flexible tubing of the resistor with respect to the high pressure (≈80 PSI) in the insulating vessel. To date, two types of ion sources have been used, as described in (*Kwan et al*., 2000). Both the contact-ionization and alumino-silicate sources produce nearly identical profiles and transverse phase space distributions at QD1. The alumino-silicate source has a much longer lifetime, which has increased the beam availability for experiments. The injector beam characterization measurements and the very first measurements through the HCX were made with the contact ionization source, before switching to the alumino-silicate source.

The six-quadrupole matching section is designed to compress the beam area transversely by a factor ≈25 and produce the matched beam parameters for periodic transport in the electrostatic lattice. In this significant beam manipulation the radii of the first (QM1) and last (QM6) matching quadrupole bores are r_p=100 mm and 31 mm respectively, and the maximum envelope excursions occur in the first and second quads, with the beam filling up to 0.8• r_p. The beam centroid exiting the injector is offset from the beam line axis by a few millimeters and milliradians, and the centroid undergoes betatron oscillations through the first three (QM1-3) quadrupoles of the matching section until being corrected in QM4-6. QM4-6 may each be displaced in the horizontal and

vertical directions by ±15mm to correct the beam centroid offset. Typical matching section voltages and displacements are indicated in Table 1. (Experiments at higher injection energy will require proportional increase in the quadrupole potentials to achieve a nearly identical envelope solution.)

Though the beam fills a relatively large fraction of the aperture in the early part of the matching section, pickup signals capacitively coupled to the quadrupole electrodes indicate beam loss is less than 0.5% through the middle, or "flat-top" of the beam pulse. The pickup signal due to lost ions is effectively amplified by the large (>10) secondary electron coefficient, making this diagnostic more sensitive to beam loss than comparisons of the Rogowski loop at the injector exit to the Faraday cup at QD1. The Rogowski-Faraday cup comparison indicates >97% current-transmission in the matching section, where the relative accuracy of this measurement is a few percent.

The three steering quadrupole displacements are determined by calculating the (single particle) centroid trajectory through QM4-6 for a misaligned beam, then solving for the required displacements. Three steering quadrupoles are used to align the beam centroid at QD1 (instead of the minimum of two displacements) subject to the additional constraint of minimizing the sum of displacements of the lenses. The phase space measurements at QD1 are shown in Fig. 2 and the horizontal and vertical profiles are in Fig 3. These preliminary envelope parameters are within ≈10% of those required for matched transport, and further tuning of the matching section will be necessary to reduce envelope mismatches downstream. The beam centroid positions (<x>, <y>) and angles (<x'>, <y'>) will also be improved.

3.2 Electrostatic quadrupole transport

For the initial round of measurements, where we have planned quiescent transport with little beam loss, the expected maximum envelope excursion of a matched beam is ≈14mm, while the aperture radius is 23 mm. The single-particle betatron phase advance is ≈67°/period, while the space-charge depressed phase advance is ≈20°/period. Since the beam is not yet well matched and has a residual centroid offset, the peak envelope excursions are probably 18-20 mm at a few places in the lattice according to envelope calculations for the data presented here. However, we have measured nearly 100% transmission of the beam according to the Faraday cup comparisons (Fig. 4) and the capacitive probes (Fig 5). The phase space measured at the end of the transport section (Fig. 6) appears to have qualitatively similar distortions from nonlinearities to that at QD1. The centroid offsets are mainly manifestations of residual offsets measured at QD1 that will be corrected in future measurements. An intensity profile of the beam at D-end is shown in Fig.7, as measured by a Kapton film exposed to the beam for ≈100 pulses. The distribution is asymmetric in the vertical plane, as is the case upstream at QD1. The beam perimeter has a diamond shape with some internal variation of intensity. Diamond-shaped beams are predicted by particle-in-cell simulations of a perfectly aligned beam at $\sigma_o = 80^o$ (*Celata et al*., 2002). The distribution is clearly asymmetric in the vertical direction, which is also observed in the slit profile measurements at this location. The measured centroid angle and position (<x>, <y>, <x'>, <y'>) accuracy is ≈0.2 mm and ≈0.2 mrad. Thus, we expect to align within that tolerance and match the beam as well as possible, then characterize the phase space at the end of the first 10 quadrupoles.

3.3 Diagnostics development

The D-end station is a venue for diagnostic development. In addition to Kapton based beam imaging, we have made progress in optical fluorescence based diagnostic techniques. We have demonstrated a scintillator material (sintered alumina) with adequate time response and lifetime for intense low-energy heavy-ion beams such as in this experiment. The optical diagnostics can produce time resolved images of the entire beam in a single pulse. The full intensity of the heavy-ion beam damages the scintillator material with an e-folding rate of ≈100 pulses. Therefore the beam must be attenuated to increase the scintillator life. Because of the high-intensity of the optical signals, attenuation is easily accomplished. The beam images are captured with an image-intensified CCD camera with an effective spatial resolution of <0.2 mm, which is set by the collection optics. The ability to gate the image intensifier to a time window <1 μs restricted to the flat-top, head or tail of the beam will allow us to characterize the transverse intensity J(x, y) in only a few Marx pulses. A prototype optical slit scanner for phase-space measurements is now being designed. This will also dramatically decrease the scanning measurement time compared to the double slit scanner diagnostic. We have also initiated a study of non-intercepting beam diagnostic capability by fluorescence imaging of the beam directly on ambient gas.

In preparation for measurements with magnetic quadrupoles, where secondary electrons and atoms due to halo scraping the beam tube are a concern, a gas and electron desorption diagnostic will be installed at the end of the beam line (*Molvik et al.,* 2002). This will determine the secondary electron and atom yields per incident ion at a shallow scattering angle.

4 SUMMARY AND FUTURE PLANS

The HCX experiment is now operational through the first 10 electrostatic quadrupoles with a 0.2 Ampere K^+ beam at 1.0 MeV. The first significant manipulation, compressing the beam transversely and delivering a matched beam to the transport section is nearly complete: With little emittance growth, the beam transmission is almost 100% and the envelope parameters are within 10% of those desired. We plan to align to within our present measurement accuracy of ±0.2 mm, match the beam as well as possible, then characterize the phase space at the end of the first 10 quadrupoles. A key question is to determine how well the beam parameters can be controlled.

Subsequently, we will parametrically vary the initial beam conditions: The centroid offset of the beam will be varied via displacements of QM4-6 to study sensitivity to alignment. The initial envelope parameters will be varied to intentionally mismatch the beam and induce halo formation, a topic under theoretical study. The first transport quadrupole, QD1, is precisely constructed to allow precise rotation about the beam axis (2^o - 4^o) for skew coupling measurements. Then all these parametric variations will be repeated at a larger fill factor by lowering the quadrupole-focusing gradient. The injected beam current will also be varied to probe the fill factor. Finally, depending on the results of these measurements, we may consider building smaller aperture quadrupoles to verify the maximum filling factor at the highest stable phase advance.

A beam line of four pulsed magnetic quadrupoles, instrumented with diagnostics to measure the production and energy of trapped electrons, secondary atoms and ions is being assembled. They will be installed after the first group of 10 electrostatic quads in the summer of 2002. In 2003 we will add 20-30 more electrostatic quadrupoles to gain

greater sensitivity to the phase space evolution of the beam, allowing more precise extrapolation to longer lattices.

In the area of longitudinal beam dynamics and control, an induction module is being built (*Burkhart et al*., 2002) which will apply agile control of the acceleration waveforms to correct for space charge field effects on the head/tail of the beam. The apparatus includes a complete system of induction cores and modulators for installation in the HCX lattice between matching section and the QD1 quadrupole. It will regulate 20kV variations during the flattop (to $\pm 0.1\% V_{injector}$) to study consequences of pulse energy variations and correct waveform imperfections. Also, ± 200kV "ear" (actively regulated to ±3%) waveforms will prevent the bunch ends from eroding due to the longitudinal self-field of the beam.

Many aspects of the HCX research and development described here and elsewhere in these proceedings are relevant to the Integrated Beam Experiment (IBX), which will accelerate one beam (eventually multiple beams) of 0.7-Ampere K^+ to 10-20 MeV in 40-100 lattice periods. The objectives of the IBX include demonstrating the injection, acceleration, compression, bending, and focusing of heavy ion beams at line charge density similar to the initial stages of a driver (*Barnard et al*., 2002). Though the physics and accelerator parameters are not yet fixed, the prototype magnetic quadrupole focusing unit (*Sabbi et al.,* 2002) and the bunch control module have many characteristics of components necessary for the IBX. Because the initial beam conditions will be similar to the HCX, the information on the maximum current that may be transported and the data analysis of the influence of secondary particles on the beam will have a direct influence on the IBX design.

REFERENCES

Barnard, J. *et al*. (2002). *these proceedings.* Integrated Experiments For Heavy Ion Fusion: IBX and IRE.

Burkhart, C. (2001) "The Closed-loop Amplifier Regulated Driver, a High Accuracy, Low Cost Modulator for HIF Accelerators," *US Dept. of Energy SBIR final Report,* DE-FG03-00ER83010, May 2001.

Celata, C.M. *et al*. (2001). PIC Simulations of Beam Dynamics Experiments Planned for the High Current Experiment *Proc. 2001 Part. Accel. Conf.* pp. 2926-2928, IEEE #01CH37268C. Piscataway, NJ 08855.

Celata, C.M. *et al*. (2002). *these proceedings.* Particle-in-Cell Simulations of Beam Dynamics in the HCX.

Faltens, A. *et al*. (2002). *these proceedings.* Development of superconducting magnets for heavy-ion fusion.

Friedman, A. *et al.* (2002). *these proceedings*. Synthesizing a 4D Beam Particle Distribution from Multiple 2D Views.

Karpenko, V. *et al*. (2001). An Engineering Overview of an Electrostatic Quadrupole Lattice for a High Current Transport Experiment *Proc. 2001 Part. Accel. Conf,* p.1447-1449, IEEE #01CH37268C. Piscataway, NJ 08855.

Kwan, J. W. *et al*. (2002). *these proceedings.* A 1.8 MeV K^+ injector for the high current beam transport experiment.

Lund, S. *et al*. (2002). *These proceedings.* Theory and Simulations in Support of the High Current Transport Experiment for Heavy-Ion Fusion.

Molvik, A.W. (2002). *these proceedings* Electron effects in intense, ion beam linacs – theory and experimental planning for HCX.

Seidl, P.A. *et al*. (2001). Overview of the Scientific Objectives of the High Current Experiment for Heavy-Ion Fusion *Proc. 2001 Part. Accel. Conf.* pp. 2932-2934, IEEE #01CH37268C. Piscataway, NJ 08855.

Tiefenback, M.G. (1987). Experimental Measurement of Emittance Growth in Mismatched Space Charge Dominated Beams *Proc. 1987 Part. Accel. Conf.* pp. 1046-1048, IEEE # 87CH2387-9, Piscataway, NJ 08855. Tiefenback, M.G. & Keefe, D. (1985). Measurement of Stability Limits for a Space-Charge-Dominated Ion Beam in a Long A.G. Transport Channel. *IEEE Trans. Nucl. Sci,* NS-32, pp. 2483-2485, Piscataway, NJ 08855.

TABLES

Table 1: Typical matching section voltages and steering offsets for operation at E_b = 1.0 MeV. Later measurements at 1.8 MeV will require ≈1.8X higher quadrupole voltages to achieve the same beam envelope.

Quadrupole	V_Q	Gradient	Clear aperture radius	x-offset	y-offset
	(kV)	(kV/cm^2)	(mm)	(mm)	(mm)
QM1	±42.8	.86	10	0	0
QM2	±32.8	.81	9	0	0
QM3	±35.98	1.0	8.5	0	0
QM4	±28.56	1.3	6.7	+0.4	+0.8
QM5	±36.15	3.0	4.9	-3.9	+1.3
QM6	±41.84	8.7	3.1	-2.0	-3.9
QD1-10	±25.5	9.6	2.3	0	0

FIGURE CAPTIONS:

Figure 1: Elevation view of the present configuration of the HCX experiment.

Figure 2: Vertical (a and b) and horizontal (c) phase space measurements at the end of the matching section. In (b), the coherent envelope divergence angle has been removed to clarify the details of the measured phase space.

Figure 3: Vertical (top) and horizontal (bottom) slit-scan profiles at the end of the matching section.

Figure 4: Capacitive monitor signals from the first and last matching section quadrupoles (QM1 and QM6).

Figure 5: Comparison of the Faraday cup data at the entrance to the transport section (QD1) to the data at the exit (D-end). The integrated beam current corresponds to 6 x 10^{12} K^+ ions/pulse.

Figure 6: Horizontal and transverse phase space measurements at the end of the first ten electrostatic quadrupoles. The lengths of the horizontal bars are proportional to the signal intensity measured at the coordinates of the right end of each bar.

Figure 7: Intensity distribution of the beam at D-end, measured with a Kapton film. The spacing between the grid lines is 5 mm.

Figure 1:

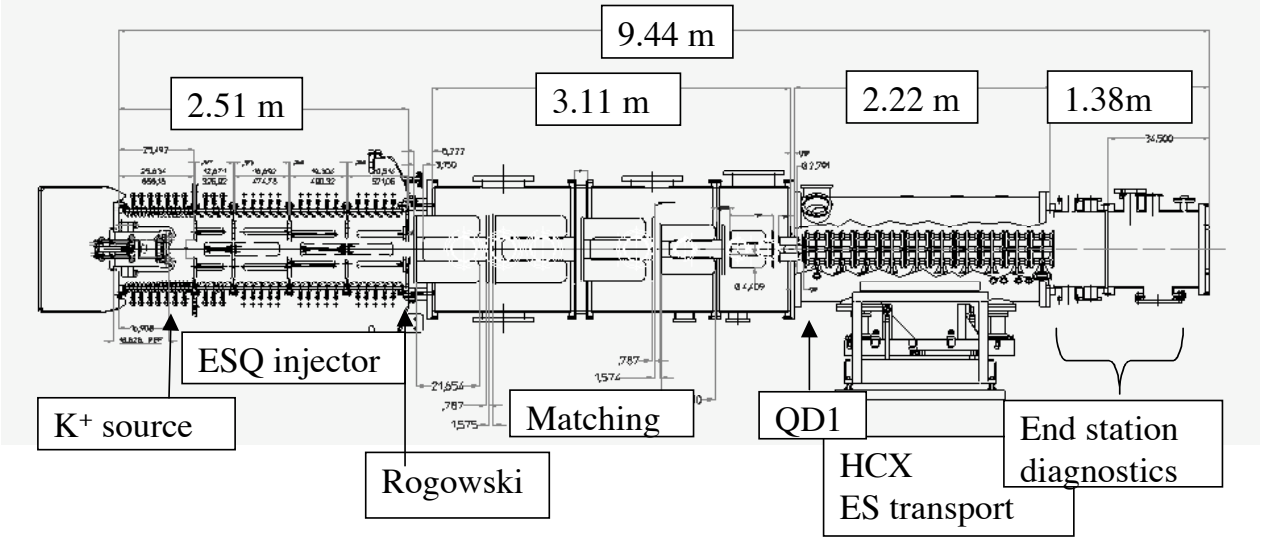
9.44 m
2.51 m
3.11 m
2.22 m
1.38m
ESQ injector
K+ source
Rogowski
Matching
QD1
HCX
ES transport
End station
diagnostics

Figure 2:

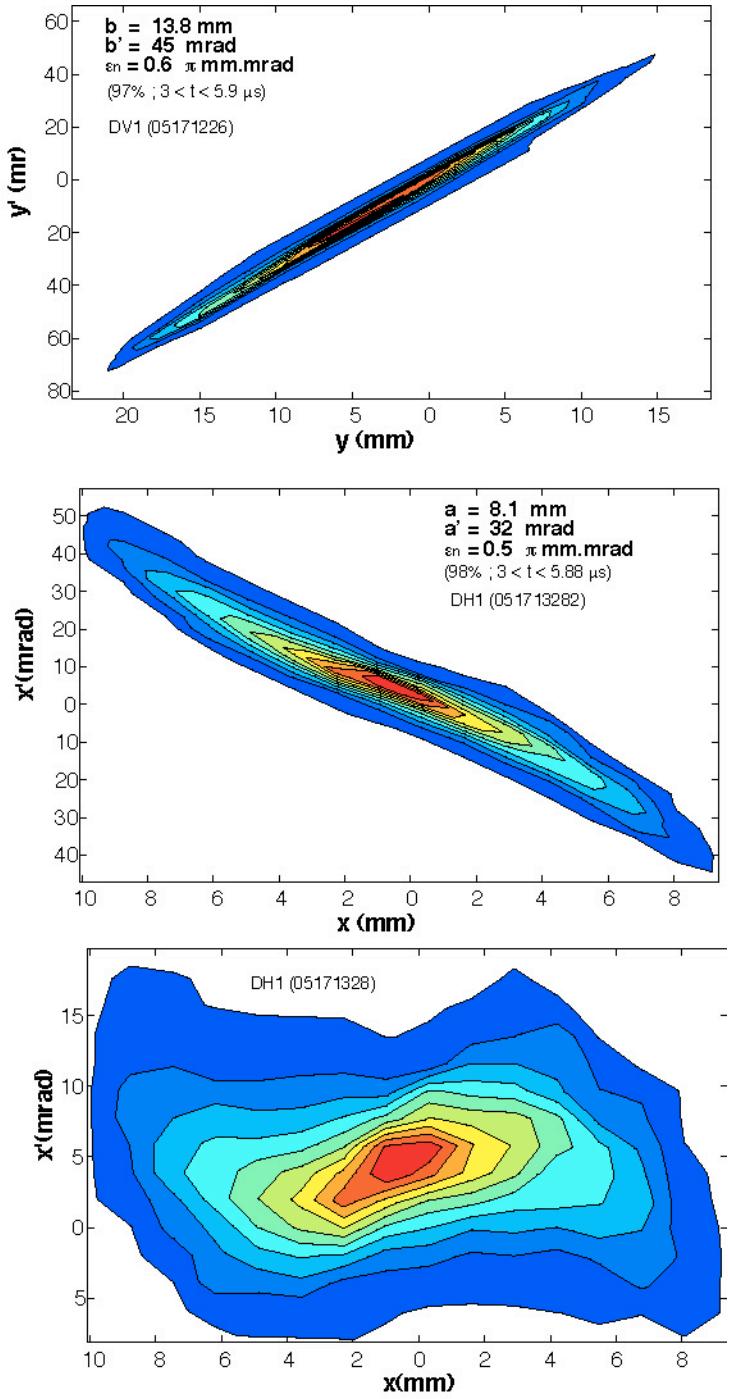
b = 13.8 mm
b' = 45 mrad
εn = 0.6 π mm.mrad
(97% ; 3 < t < 5.9 μs)
DV1 (05171226)
y' (mr)
y (mm)
a = 8.1 mm
a' = 32 mrad
εn = 0.5 π mm.mrad
(98% ; 3 < t < 5.88 μs)
DH1 (051713282)
x'(mrad)
x (mm)
DH1 (05171328)
x'(mrad)
x(mm)

Figure 3:

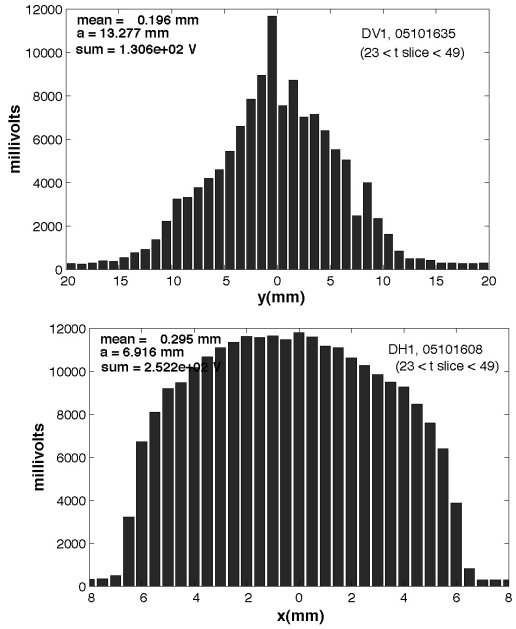
mean = 0.196 mm
a = 13.277 mm
sum = 1.306e+02 V
DV1, 05101635
(23 < t slice < 49)
millivolts
y(mm)
mean = 0.295 mm
a = 6.916 mm
DH1, 05101608
(23 < t slice < 49)
millivolts
x(mm)

Figure 5:

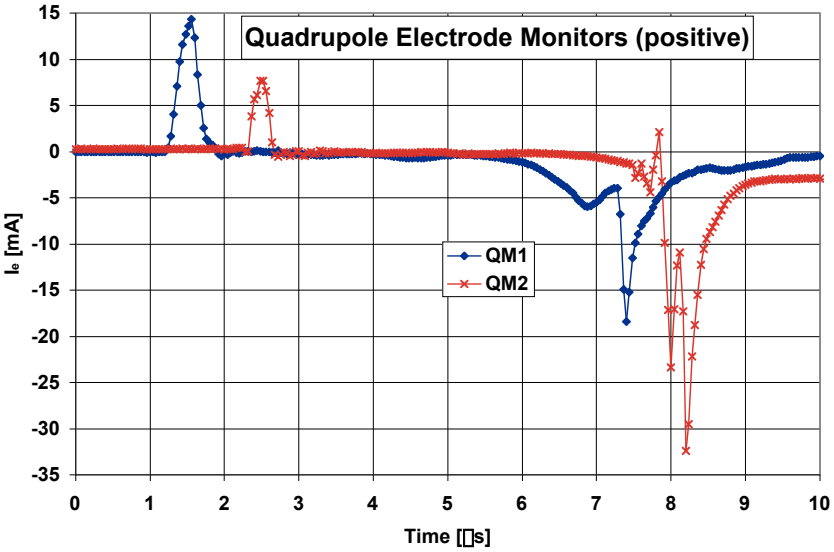
Quadrupole Electrode Monitors (positive)
QM1
QM2
Ie [mA]
Time [□s]
15
10
5
0
-5
-10
-15
-20
-25
-30
-35
0
1
2
3
4
5
6
7
8
9
10

Figure 4:

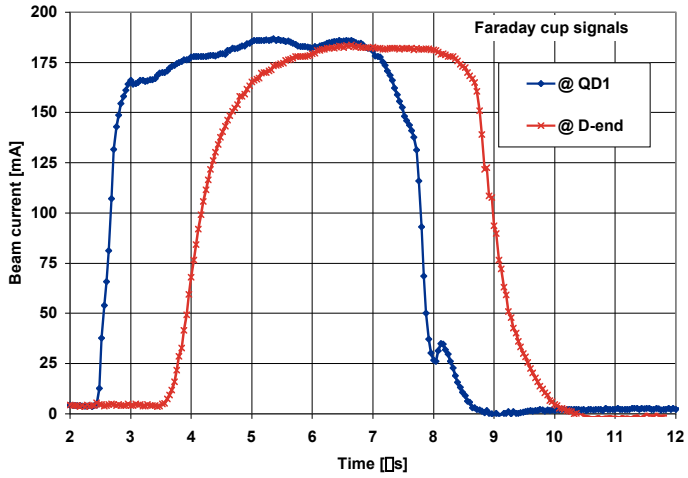
Faraday cup signals
@ QD1
@ D-end
Beam current [mA]
Time [μs]
200
175
150
125
100
75
50
25
0
2
3
4
5
6
7
8
9
10
11
12

Figure 6:

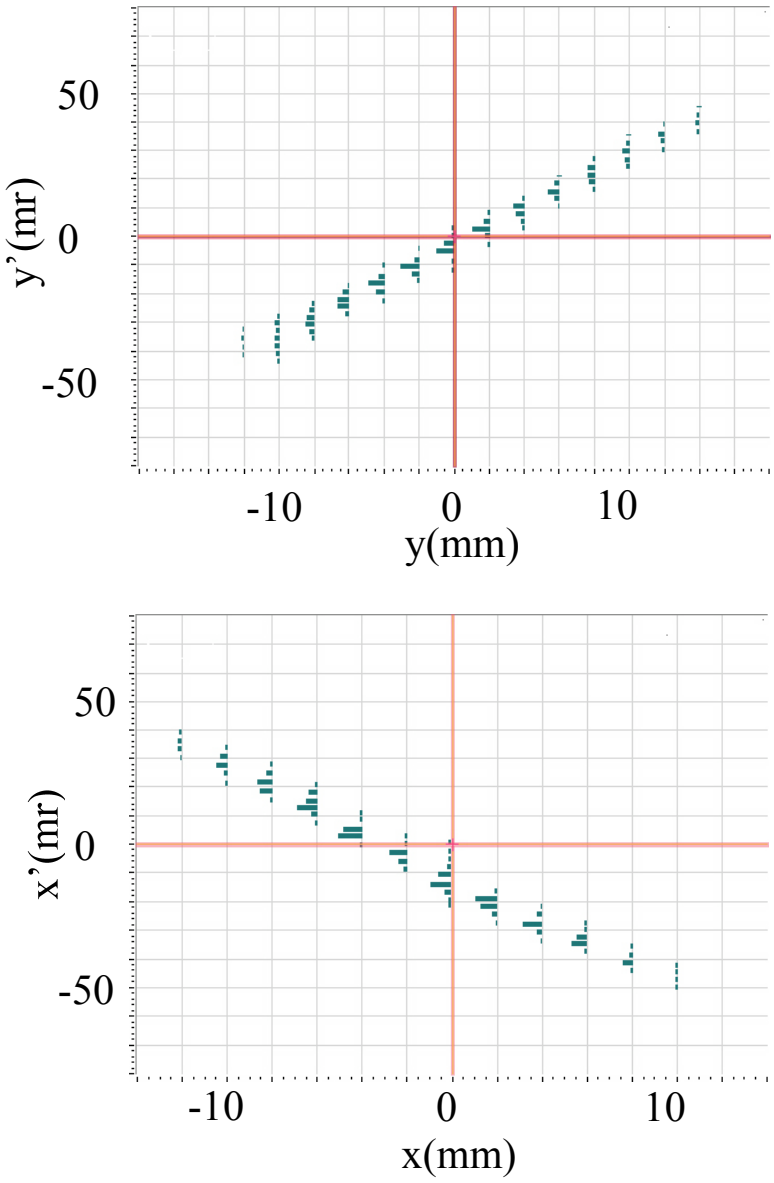

Figure 7: